INSTITUTE OF PHYSICS PUBLISHING SEMICONDUCTOR SCIENCE AND TECHNOLOGY
Semicond. Sci. Technol. **20** (2005) 621–624 doi:10.1088/0268-1242/20/6/024

High-power 808 nm lasers with a super-large optical cavity

A Knauer, G Erbert, R Staske, B Sumpf, H Wenzel and M Weyers

Ferdinand-Braun-Institut für Höchstfrequenztechnik, Gustav–Kirchhoff–Str. 4, 12489 Berlin, Germany

E-mail: knauer@fbh-berlin.de

Received 2 March 2005, in final form 4 April 2005
Published 27 April 2005
Online at stacks.iop.org/SST/20/621

Abstract
We present a detailed design and experimental study of diode laser structures emitting at 808 nm based on the combination of a GaAsP quantum well with well-established AlGaAs waveguide structures. By increasing the thickness of the confinement layers of the laser structure, its vertical far field divergence is reduced down to 15° with only a small increase of the threshold current and small loss of efficiency. 200 μm aperture 'broad area' devices achieve at a heat sink temperature of 25 °C a continuous wave (CW) output power of more than 15 W with a wall-plug efficiency of 50% with a vertical far field divergence of 18°. This output power illustrates the excellent high-power performance by using super-large optical-cavity structures with improved beam characteristics in comparison to the conventional broad waveguide lasers.

1. Introduction

High-power diode lasers emitting at 808 nm find widespread applications as pump sources for Nd:YAG solid-state lasers. Presently, there are big efforts underway to improve the operational characteristics of these diode lasers in order to reduce the costs per watt output power. For example, a high wall-plug efficiency and a low temperature sensitivity allow the use of passively conduction-cooled instead of actively water-cooled heat sinks. Another option which is investigated in this paper is the reduction of the vertical far field divergence to a full width at half maximum (FWHM) below 20° which permits the application of optical elements with a small numerical aperture. An additional effect is the increase of the mode size resulting in a reduced optical power density. This raises the power level where catastrophic optical damage (COD) occurs, thus increasing the lifetime.

Unfortunately, a decrease of the confinement factor is inevitably connected with a deterioration of the laser performance, such as threshold current, slope efficiency or maximum output power. In order to minimize this, several approaches were proposed in the literature [1–4]. Two major schemes can be distinguished: either a low-index layer is inserted into the confinement layer, or a high-index layer is inserted into the cladding layer. In [5], an alternative approach was presented, where the usual confinement layers were omitted and instead the confinement of the optical field was provided by high-index quarter-wave reflecting layers inserted into the cladding layers. Later this concept was extended in [6], where a very (>14 μm) thick periodic multilayer structure was employed.

High-power operation of 808 nm single-stripe emitters and laser bars having a similar AlGaAs-based structure with GaAsP active region as the devices investigated in this paper was already demonstrated in [7]. A COD power level of 9 W was obtained with a 100 μm stripe-width device. A cm-bar having a filling factor of 28% exhibited a maximum output power of 148 W. The devices had already a narrow vertical far field divergence (26° FWHM). Here, we investigate the possibility of a further decrease of the far field divergence by simply increasing the thickness of the confinement layers, keeping the excellent high-power performance.

Details of the structure and theoretical considerations are presented in section 2. The fabrication process is described in section 3. Experimental results obtained under pulsed operation and in continuous wave (CW) mode are given in section 4. Finally, the results are summarized in section 5.

2. Theoretical considerations

The laser structure investigated in this study consists of n- and p-doped $Al_{0.70}Ga_{0.30}As$ cladding and $Al_{0.45}Ga_{0.55}As$

 © 2005 IOP Publishing Ltd Printed in the UK

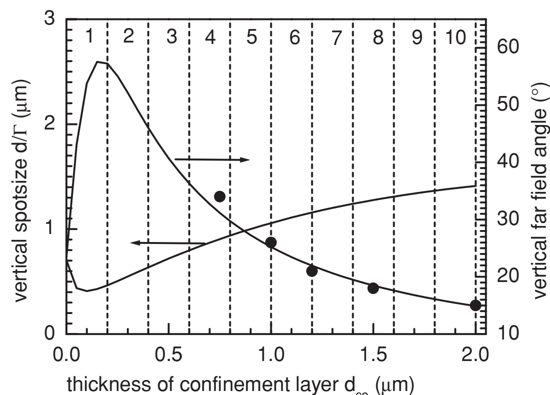

Figure 1. Calculated equivalent vertical spotsize (left axis) and vertical far field angle (FWHM, right axis) versus the thicknesses of the confinement layers simultaneously varied on each side of the SQW. The vertical dashed lines separate the regions with the numbers of modes given on top. Thickness of active region is 14 nm. Bullets: experimental far field angles.

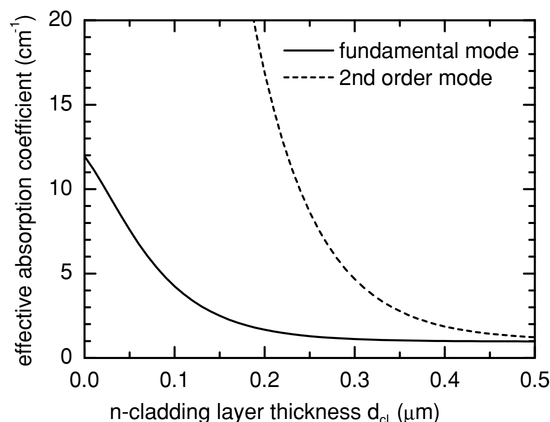

Figure 2. Calculated optical losses of the fundamental mode (solid) and second higher order mode (dashed) for a confinement layer thickness of 1.5 μm.

confinement layers. The undoped active region, a tensile-strained 14 nm thick GaAsP single quantum well (SQW), is sandwiched between the confinement layers having the same thickness d_{co}. The layer structure is completed by a highly p-doped GaAs contact layer. All heterojunctions are graded in order to reduce the serial resistance. More details of the structure and the properties of the GaAsP SQW can be found in [8].

Figure 1 depicts the calculated dependence of the equivalent vertical spotsize d/Γ ($d = 14$ nm, Γ confinement factor of active region) and the vertical far field angle (FWHM) of the fundamental transverse-magnetic (TM) mode on the thicknesses of the confinement layers simultaneously varied on each side of the SQW. Due to the fact that here the total width of the waveguide core which is twice the value of d_{co} is more than a factor of 2 larger than that of usual broadened waveguide structures [9], we call them 'super-large optical-cavity' (SLOC) structures. If d_{co} is enlarged from 0.75 μm to 2 μm, the d/Γ value increases from 0.9 μm to 1.4 μm and the far field angle decreases from 31° to 15°. However, at the same time more and more modes are guided. The number of guided modes is also indicated in figure 1. Normally these modes will not lase because the confinement factors of the even higher order modes are much smaller than those of the fundamental modes. The confinement factors of the odd modes vanish anyway. Furthermore, in the case of TM polarization, the facet reflectivity decreases with rising mode order which shifts the necessary threshold gain to larger values, too.

In order to facilitate the discrimination of the higher order modes, the thickness of the cladding layers can be chosen such that the optical losses of the higher order modes due to radiation into the substrate are much larger than those of the fundamental mode. This is shown in figure 2 for $d_{co} = 1.5\ \mu$m where the effective absorption coefficient (proportional to the imaginary part of the propagation constant) containing both contributions due to absorption (limit $d_{cl} \to \infty$) and radiation is plotted versus the thickness of the n-cladding layer. The difference in the losses between the fundamental and second-order mode is about 2 cm^{-1} for $d_{cl} = 0.35\ \mu$m which is sufficient for discrimination. A minimization of the cladding layer thicknesses has the additional positive effect of a reduction of the electrical and thermal resistances.

3. Fabrication

The AlGaAs/GaAsP layer structures were grown by metal-organic vapour-phase epitaxy at 750 °C and a pressure of 70 hPa in a horizontal reactor (AIX200/4) using TMGa, TMAl, DMZn, PH_3, AsH_3 and disilane as precursors on (0 0 1) exact-oriented GaAs substrates. Note that because of the small confinement factor and the correspondingly large threshold carrier density, the precursors especially TMAl and AsH_3 must be carefully selected with respect to their purity in order to ensure a low density of non-radiative recombination centres in the epitaxial layers [10]. Thickness, composition and strain (ε) of the layers were controlled by scanning electron microscopy and high resolution X-ray diffraction in (0 0 4) reflection.

Broad area (BA) lasers with stripe widths of 100 μm and 200 μm and cavity lengths of 1 mm and 4 mm were manufactured by etching away the contact layer beyond the stripe p-electrode followed by sputtering of an insulator. For CW measurements, 4 mm long AR/HR (2%/90%) facet-coated devices were soldered p-side down on CuW submounts by exploiting the AuSn ζ phase [11]. The n-side was contacted by wire bonding.

The submounts were mounted with PbSn solder on heat sinks. In contrast to standard mounting on C-mount, a specially designed conduction cooled package (CCP) was used. The standard C-mount used for single emitters has dimensions of 6.4 × 6.8 × 4.2 mm^3. Depending on the size of the diode lasers a thermal resistance between 5 and 8 K W^{-1} is obtained. This value limits the reliable output power to about 5 W. The dimensions of the CCP are 25 × 25 × 7.6 mm^3, comparable to packages used for cm-laser bars and designed for power loads up to 50 W.

4. Experimental results

Owing to the tensile-strained active region ($\varepsilon \approx 0.57\%$), the lasing emission is TM polarized. The influence of the design variations on the electro-optical laser parameters was studied

Table 1. Compilation of data obtained under pulsed operation of as-cleaved devices. Stripe width is $W = 100\ \mu$m.

Structure	d_{co} (μm)	d_{cl} (μm)	$L = 1$ mm Θ (°)	I_{th} (mA)	S (W A^{-1})	η_d (%)	T_0 (K)	j_{tr} (A cm^{-2})	$\Gamma \cdot g_0$ (cm^{-1})	η_i (%)	α_i (cm^{-1})
A	0.75	0.7	34	279	0.694	90	106	141	17.7	97	1.0
B	1.0	0.5	26	291	0.665	86	102	138	16.0	95	1.1
C	1.2	0.4	21	314	0.663	86	100	140	14.8	92	0.8
D	1.5	0.35	18	354	0.645	84	90	148	13.2	88	0.7
E	2.0	0.3	15	402	0.616	80	84	149	11.8	87	0.7

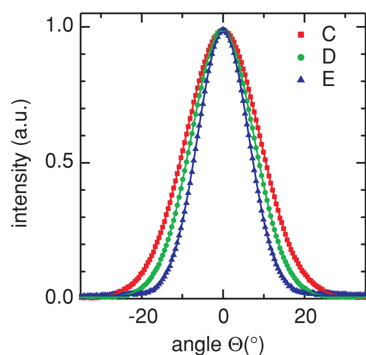

Figure 3. Vertical far field profiles of structures C, D and E of table 1. Symbols: experimental values. Solid lines: Gaussian fits.

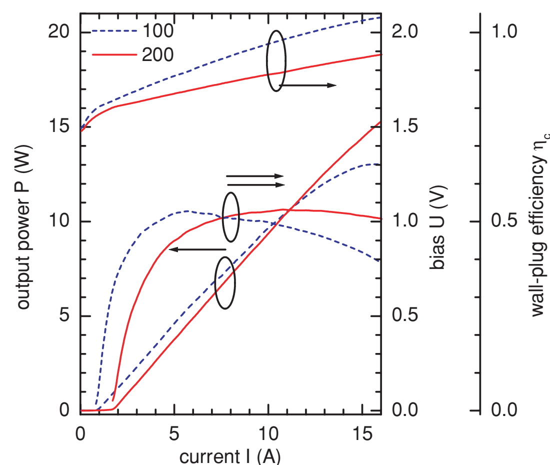

Figure 4. CW output power (left axis), bias (right axis) and conversion efficiency (right-most axis) versus injection current of 4 mm long lasers having structure D mounted p-down on CCP. The stripe widths are 100 μm (dashed) and 200 μm (solid). Heat sink temperature is 25 °C.

on uncoated devices with a stripe width of 100 μm. The power–current characteristics and its temperature dependence as well as the far field distribution of devices with varying cavity lengths L were measured in pulsed mode (1 kHz repetition rate, 1 μs pulse duration).

The results are compiled in table 1. The second and third columns there give the thicknesses of the p- and n-doped confinement and cladding layers, respectively. The vertical far field angle Θ (FWHM), threshold current I_{th}, slope efficiency S, differential external efficiency η_d and the characteristic temperature T_0 of the threshold current are given for 1 mm long devices in columns 4–8. On the basis of a logarithmic dependence of the current on the gain, from the dependences of $\log(I_{th}/L)$ on L and $1/\eta_d$ on $1/L$ the figures of merit transparency current density j_{tr}, modal gain coefficient $\Gamma \cdot g_0$, internal efficiency η_i and the internal losses α_i were determined, using a facet reflection coefficient of 30%.

As the calculations shown in figure 1 predict, the vertical far field angle goes down to 15° for structure E ($d_{co} = 2\ \mu$m). The increase of the threshold current by a factor of 1.4 is mainly caused by a reduction of the modal gain coefficient by a factor of 0.7 in agreement with the calculations. The decrease of the slope efficiency (and the external differential efficiency) by only a factor of 0.9 is caused by a reduction of the internal efficiency by the same factor which might be, similar to the decrease of the T_0 value, related to an increased excess carrier density in the confinement layers due to the larger spacing of the quasi-Fermi energies. The transparency current density mainly characterizing the QW increases and the internal losses decrease only slightly with the broadening of the waveguide. The latter dependence was already found, although more pronounced, by others [12].

The vertical far field profiles of structures C, D and E are shown in figure 3. The nearly Gaussian shapes of the profiles as revealed by the fits greatly simplify the coupling of the laser emission into optical systems. This is in contrast to other approaches (compare, for example, [13]), where the far field often has substantial side lobes or shoulders at larger angles.

The parameters even for the layer structure E with the smallest far field angle of 15° are still promising for a manufacturing of laser devices. However, for an evaluation of the high-power performance in the following, we will present CW results for devices having structure D with $d_{co} = 1.5\ \mu$m (total waveguide core 3 μm), mounted p-down on CCP as described in section 3 and stabilized at a temperature of 25 °C.

The power–current, voltage–current and efficiency–current characteristics of 4 mm long lasers with stripe widths of 100 μm and 200 μm are shown in figure 4. It can be seen that the 100 μm device achieves a maximum output power of 13 W at an injection current of 16 A limited by thermal rollover. At the same current, the 200 μm device emits 15.3 W without thermal rollover. Thus, even a higher maximum power could be expected. The maximum conversion efficiency of both devices is nearly 0.53. However, this value is reached at 11 A (10.5 W) with the 200 μm device, whereas it is already reached at 6 A (5.5 W) with the 100 μm device. Up to these power levels, the slope efficiency of both devices is as high as 1.1 W A^{-1}, despite the long cavity.

The lateral far field angle ($1/e^2$ width) determined at 1 W, not shown here, is about 4° for the 100 μm device which

is much smaller than that of a similar 2 mm long device having structure B (7.5°) [14]. All these data illustrate the excellent features of the SLOC devices, which show data comparable to those of conventional broad-waveguide lasers but with improved beam characteristics.

5. Summary

The thicknesses of the AlGaAs confinement layers of diode lasers having a GaAsP SQW for emission at 808 nm have been optimized with respect to a small vertical far field divergence and a high-power performance. With a so-called super-large optical cavity, perfectly Gaussian-shaped vertical far field profiles with angles down to 15° (FWHM) have been obtained. At the same time, the determined deterioration of the laser performance is sufficiently small for a use in high-power laser devices. The experimentally demonstrated 13 W CW optical power from a 100 μm stripe-width device is higher than the reported COD level for comparable conventional LOC structures. Thus the reduced optical power density in the SLOC structures leads to devices with higher maximum optical output power. Reliability tests are ongoing.

Acknowledgments

The authors wish to thank M Gielow and A Krause for assistance in epitaxy and electro-optical characterization, respectively. This work was supported in part by the European Commission under project www.bright.eu contract 511722.

References

[1] Temmyo J and Sugo M 1995 *Electron. Lett.* **31** 642
[2] Verdiell J M, Ziari M and Welch D F 1996 *Electron. Lett.* **32** 1817
[3] Vakshoori D, Hobson W S, Han H, Lopata J, Henein G E, Wynn J D, Dejong J, Schnoes M L and Zydzik G J 1996 *Electron. Lett.* **32** 1007
[4] Lin G, Yen S T, Lee C P and Liu D C 1996 *IEEE Photon. Technol. Lett.* **12** 1588
[5] Wenzel H, Bugge F, Erbert G, Hülsewede R, Staske R and Tränkle G 2001 *Electron. Lett.* **37** 1024
[6] Maximov M V, Shernyakov Y M, Novikov I I, Shchukin V A, Shamid I and Ledentsov N N 2003 *J. Electron. Mater.* **39** 1729
[7] Sebastian J, Beister G, Bugge F, Buhrandt E, Erbert G, Hansel H G, Hülsewede R, Knauer A, Pittroff W, Staske R, Schröder M, Wenzel H, Weyers M and Tränkle G 2001 *IEEE J. Sel. Top. Quantum Electron.* **7** 334
[8] Wenzel H, Erbert G, Bugge F, Knauer A, Maege J, Sebastian J, Staske R, Vogel K and Tränkle 2000 *Proc. SPIE* **3947** 32
[9] Botez D 1999 *Appl. Phys. Lett.* **74** 3102
[10] Knauer A, Wenzel H, Erbert G, Sumpf B and Weyers M 2001 *J. Electron. Mater.* **70** 1421
[11] Pittroff W, Erbert G, Beister G, Bugge F, Klein A, Knauer A, Maege J, Ressel P, Sebastian J, Staske R and Tränkle G 2001 *IEEE Trans. Compon. Packag. Manuf. Technol.* B **24** 434
[12] Garbuzov D Z, Ables J H, Morris N A, Harvey M G and Connolly J C 1996 *Proc. Conf. on Lasers and Electro-Optics (Anaheim)* p 79
[13] Xu Z, Gao W, Siskavich B, Nelson A, Cheng L, Luo L, Kim H S, Wang Z and Chin A K 2004 *Proc. SPIE* **5365** 142
[14] Hülsewede R, Sebastian J, Wenzel H, Beister G, Knauer A and Erbert G 2001 *Opt. Commun.* **192** 69